Metal(loid) bioaccessibility and inhalation risk assessment: a comparison between an urban and an industrial area

A. Hernández-Pellón[a*], W. Nischkauer[b], A. Limbeck[b] and I. Fernández-Olmo[a]

[a] Dpto. de Ingenierías Química y Biomolecular, Universidad de Cantabria, Avda. Los Castros s/n, 39005 Santander, Cantabria, Spain
[b] TU Wien, Institute of Chemical Technologies and Analytics, Getreidemarkt 9/164-IAC, A-1060 Vienna, Austria

*Corresponding Author
Dpto. de Ingenierías Química y Biomolecular, Universidad de Cantabria, Avda. Los Castros s/n, 39005 Santander, Cantabria, Spain
ana.hernandez@unican.es

Abstract

The content of metal(loid)s in particulate matter (PM) is of special concern due to their contribution to overall (PM) toxicity. In this study, the bioaccessibility and human health risk of potentially toxic metal(loid)s associated with PM_{10} were investigated in two areas of the Cantabrian region (northern Spain) with different levels of exposure: an industrial area mainly influenced by a ferromanganese alloy plant; and an urban area consisting mainly of residential and commercial activities, but also affected, albeit to a lesser extent by the ferroalloy plant. Total content and bioaccessible fractions in simulated lung fluids (SLFs) of Fe, Mn, Zn, Ni, Cu, Sb, Mo, Cd and Pb were determined by ICP-MS. Gamble's solution and artificial lysosomal fluid (ALF) were used to mimic different conditions inside the human respiratory system. A health risk assessment was performed based on the United States Environmental Protection Agency's (USEPA) methodology. Most metal(loid)s showed moderate and high bioaccessibility in Gamble's solution and ALF, respectively. Despite the high variability between the samples, metal(loid) bioaccessibility was found to be higher on average at the industrial site, suggesting a greater hazard to human health in the proximity of the main metal(loid) sources. Based on the results of the risk assessment, the non-carcinogenic risk associated with Mn exposure was above the safe limit (HQ>1) under all the studied scenarios at the industrial site and under some specific scenarios at the urban location. The estimated carcinogenic inhalation risk for Cd exposure at the industrial site was found to be within the range between 1.0×10^{-6} to 1.0×10^{-4} (uncertainty range) under some scenarios. The results obtained in this study indicate that Mn and Cd inhalation exposure occurring in the vicinities of the studied areas may pose a human health risk.

Keywords

In vitro bioaccessibility, PM_{10}, metal(loid)s, inhalation risk assessment, ferroalloy plant

1. Introduction

Atmospheric particulate pollution is an increasing cause of concern for human health, especially in urban and industrialized areas. It is implicated in a wide variety of cardiovascular (Brook et al., 2010; Fiordelisi et al., 2017; Hoek et al., 2013) and respiratory diseases (Noh et al., 2016; Taj et al., 2017), including lung cancer (Raaschou-Nielsen et al., 2013). Additionally, numerous epidemiological studies have associated particulate matter (PM) exposure with reproductive problems (Carré et al., 2017) and neurodevelopmental and neurodegenerative diseases (Wang et al., 2017).

The potentially adverse health effects from the inhalation of PM depend on its physico-chemical characteristics (Kelly and Fussell, 2012), which vary significantly in urban, industrial and rural areas around the world (Mukherjee and Agrawal, 2017). Transition metals are of particular interest for the assessment of PM toxicity, due to the fact that they are capable of generating reactive oxygen species (ROS) (Verma et al., 2010), which induce inflammatory responses, DNA damage and oxidative stress (Peixoto et al., 2017; Van Den Heuvel et al., 2016). Many of these metals are emitted by industrial activities such as Al, Fe, Zn, Mn and Pb by the integrated steel industry (Hleis et al., 2013; Sylvestre et al., 2017; Yatkin and Bayram, 2008), Mn by the ferroalloy industry (Haynes et al., 2010; Lucas et al., 2015; Mbengue et al., 2015; Menezes-Filho et al., 2016), As and Cu by Cu smelters (Chen et al., 2012; Sánchez de la Campa et al., 2011) and Zn, Cd and Pb by Zn smelters (MacIntosh et al., 2010). An evaluation in terms of exposure and potential health risks for local residents is vital when these activities are located close to urban areas.

The identification of the true harmful components of PM, i.e. those potentially able to cause adverse health effects via inhalation, is a critical goal for toxicological studies (Kelly and Fussell, 2012). The toxicity of metal(loid)s in PM or dust upon uptake into the human lung is usually evaluated using one of three main approaches: 1) In-vivo methods using lab animals 2) In-vitro methods using cultured cells and 3) In-vitro methods using simulated lung fluids (SLF)s. Both in-vivo animal studies and in-vitro exposure to culture cells are complex and expensive. Therefore, in-vitro methods using SLFs are considered to be a streamlined and inexpensive alternative for toxicological studies (Kastury et al., 2017).

In this approach, the soluble metal(loid) fraction extracted with the SLFs is used as an estimation of the metal(loid) bioaccessible fraction, i.e. the amount of metal(loid) that actually interacts with the organism's contact surface and is potentially available for

absorption by the organism (US EPA, 2007). Although this approach has been applied in many works, the lack of standardized methods hinders interstudy comparisons (Guney et al., 2016; Wiseman, 2015). Significant methodological differences exist in the leaching agents employed, as well as in particle size and assay parameters, namely extraction time, liquid to solid (L/S) ratio, temperature and agitation (Caboche et al., 2011; Mukhtar and Limbeck, 2013; Wiseman, 2015). One-step or sequential extraction methods using water or simple chemicals as leaching agents have been widely applied to in-vitro metal(loid) dissolution studies (da Silva et al., 2015; Heal et al., 2005; Majestic et al., 2007; Mugica-Álvarez et al., 2012; Niu et al., 2010; Tessier et al., 1979; Voutsa and Samara, 2002). However, in the last decade, there has been a shift to physiologically based extraction techniques using SLFs as leaching agents (Boisa et al., 2014; Caboche et al., 2011; Henderson et al., 2014; Pelfrêne et al., 2017). The most commonly used SLFs are Gamble's solution and artificial lysosomal fluid (ALF). Gamble's solution (pH=7.4) is representative of the interstitial fluid in the deep lung, whereas ALF (pH=4.5) represents the more acidic intracellular conditions found in the lysosomes of alveolar macrophages (Mukhtar and Limbeck, 2013). Most of these studies focused on assessing the bioaccessibility of metal(loid)s in certified reference materials or commercial products (Caboche et al., 2011; Colombo et al., 2008; Midander et al., 2007; Pelfrêne et al., 2017) or the comparison between metal(loid) bioaccessibility in different SLFs or PM size fractions (Coufalík et al., 2016; Mukhtar et al., 2015; Potgieter-Vermaak et al., 2012; Wiseman and Zereini, 2014), with most of them being conducted in urban areas. Only a few of these studies evaluate the influence of specific industrial activities (Huang et al., 2018; Mbengue et al., 2015). Additionally, the methodology for the selection of the appropriate extraction fluid type in combination with the particle size is rarely discussed in the literature. According to Mukhtar and Limbeck (2013), particles in the range of 2.5-10 μm are in most cases deposited in the pharyngeal and tracheal region, and transported by the mucociliary clearance adoral and swallowed, thus reaching the gastrointestinal tract; while particles less than 1 μm can reach the alveolar lung regions and interact with the lung fluid. In contrast, Wiseman (2015) considers that particles smaller than 5 μm reach the pulmonary region of the respiratory tract where they are more likely to dissolve in lung fluids or be phagocytized by resident macrophages. In this regard, as Wiseman (2015)

notes, more attention should be paid to the implications of the particle size and to the appropriate selection of the SLF.

The health risk assessment associated with the inhalation route has been traditionally based on the total metal(loid) content. As a result of this and according to Huang et al. (2018), the exposure risk of metal(loid)s in PM may be overestimated. In this regard, the current trend in exposure assessment and risk calculation methods is shifting towards determining the bioaccessibility fraction of the studied metals(loids) in SLFs (Huang et al., 2018, Huang et al., 2016, Huang et al., 2014, Kastury et al., 2017).

The aim of this work is to assess the bioaccessibility of potentially toxic metal(loid)s (i.e. Fe, Mn, Zn, Ni, Cu, Sb, Mo, Cd and Pb) associated with PM_{10} collected in the Cantabrian region (northern Spain), whose presence in the air has been mainly attributed to local industries and other anthropogenic activities. In this regard, a ferroalloy plant has been identified as the main metal(loid) source in the area (mainly Mn, Fe, Zn, Cd and Pb), followed by vehicular traffic (main tracers Cu, Fe, Sb and Mo) and to a minor extent oil combustion processes (main tracers Ni and V) (Hernández-Pellón and Fernández-Olmo, 2017). Additionally, a steel plant has been found to contribute to Zn, Cu, Cd and Pb levels (Arruti et al., 2011). The differences in metal(loid) bioaccessibility at different distances from the main metal(loid) sources will be evaluated by studying two different sites: an urban-industrial area mainly influenced by the presence of a ferromanganese alloy plant; and an urban area with a lower impact from local industrial emissions, which is mostly comprised of residential and commercial activities, but also affected to a lesser extent by the ferroalloy plant. The health risk via the inhalation route will be calculated based on both the total and the bioaccessible concentrations of the studied metal(loid)s, and the limitations of these calculations will be addressed.

2. Materials and methods

2.1. Area of study

The area of study of this work is located in the north of Spain, in the Region of Cantabria (580,140 inhabitants, 2017), specifically along the Santander Bay. This study has been conducted in two locations:

1) Santander (172,656 inhabitants, 2016), which is located in the northern part of the Bay, is the most populated city of the Region, being mainly commercial and residential. The sampling site (ETSIIT, UTM, 30T, X=435450, Y=4813651, 7 m a.s.l.) is situated on the campus of the University of Cantabria, on the rooftop of the "E.T.S de Ingenieros Industriales y de Telecomunicaciones" building (30 m above ground) and represents an urban background site.
2) Maliaño (9,440 inhabitants, 2016), is a town located alongside the southern part of the Bay. It is highly impacted by nearby industrial activities, such as steel, ferromanganese and silicomanganese production. The sampling site (Vidriera, UTM, 30T, X = 431899, Y =4807290, 5 m a.s.l.) is located on the rooftop of the "Cultural Center of La Vidriera" (8 m above ground) some 350 m north of a manganese alloy production plant, and therefore represents an urban-industrial site. The presence of this plant in Maliaño has been previously associated with high concentrations of Mn in the air (Moreno et al., 2011; Ruiz et al., 2014).

The location of the monitoring sites and the main metal(loid) sources is shown in Figure S1.

2.2. Sampling and filter preparation

A PM_{10} sampling campaign was carried out at the two selected monitoring sites. A previous study showed that most of the particle types identified in PM_{10} filters collected at the Vidriera site had mean diameters of less than 2.5 μm (Hernández-Pellón et al., 2017). PM_{10} samples were collected by means of a low volume sampler device (2.3 m^3/h), equipped with a 15 filter cartridge, on 47 mm Teflon filters (PALL). This substrate was selected in order to minimize possible sample loss due to sorption of particles in the filters (Zereini et al., 2012) and because of the lower amount of metal(loid) impurities (Karanasiou et al., 2005). Twenty daily samples were collected at the Vidriera site from January to February 2017. Later, 20 additional daily PM_{10} samples were collected from February to March 2017 at the ETSIIT site.

Once the gravimetric determination was performed, the filters were cut into three pieces using ceramic scissors: one quarter of the filter was used for the total metal(loid) content analysis, while the remaining portion of the filter was cut into two equal pieces in order to assess the bioaccessible levels of the metal(loid)s.

2.3. Total metal(loid) content digestion procedure

The digestion was carried out in a 24 slot heating plate equipped with 10 ml closed PFA vessels. One quarter of each filter was treated for 60 minutes at 90ºC with a mixture of 3 ml of 65% HNO_3, 1.5 ml of 30% H_2O_2 and 50 µl of HF. The reagents used were of analytical grade or higher purity. The concentrated HNO_3, H_2O_2 and HF were sourced from Merck. After sample digestion, the non-dissolved sample constituents were separated by filtration, then the clear solution was diluted to a final volume of 30 ml with HNO_3 (0.5%) and stored refrigerated until further use (4ºC, maximum storage time 48h).

2.4. Inhalation bioaccessibility tests

The assessment of the bioaccessible fraction of metal(loid)s was performed using two SLFs as leaching agents: Gamble's solution (pH=7.4±0.1) and ALF (pH=4.5±0.1). Prior to the bioaccessibility tests, both fluids were freshly prepared using ultrapure water and analytical grade reagents provided by Merck and Sigma Aldrich. The composition and order of addition of the reagents is presented in Table 1. The pH of the SLFs was measured immediately before the beginning of the bioaccessibility test. In this study, only HNO_3 was used for pH adjustment. The use of NaOH was avoided in order to maintain the original composition of the SLFs (Wiseman and Zereini, 2014).

Due to the lack of standardized methods for the assessment of metal(loid) bioaccessible fractions in PM, the volume of SLF was established as a compromise between: 1) The use of an L/S ratio between 500-50,000 to assure that this parameter does not influence significantly the metal(loid) bioaccessibility (Caboche et al., 2011), 2) The use of a low volume of fluid to obtain a concentrated solution (beneficial for the subsequent measurement step) and 3) Ensuring suitable contact between the piece of filter and the fluid. Sample weights of the PM_{10} samples collected at the ETSIIT and Vidriera sites, ranged from 0.6 mg to 2.4 mg and from 0.6 mg to 3.1 mg, respectively. After several tests, 2 ml of SLF was selected as the minimum volume of fluid required to assure the correct contact between filter and fluid. The L/S ratios used for the determination of the metal(loid) bioaccessible fraction in SLFs were between 2244 and 8708 and between 1851 and 11007 at the ETSIIT and Vidriera sites, respectively. These L/S ratios are in the range proposed by Caboche et al. (2011) for assessing the bioaccessibility of metal(loids) in SLFs, without the risk of saturation of the solution or competition between the soluble elements.

In-vitro bioaccessibility tests were performed by introducing each portion of the filter into a 10 ml PFA vessel and adding 2 ml of the SLF. Moreover, leaching experiments were performed for 24h to avoid incomplete extractions (Caboche et al., 2011). Finally, a heating plate was used to maintain the temperature at 37ºC in order to simulate the temperature of the human body. The samples were manually agitated several times per day in a consistent manner during the extraction period. After the bioaccessibility test was performed, the samples were centrifuged at 3030 x g for 10 minutes for separation of the remaining particulate sample material and the supernatant solution was acidified; the solutions were then stored until analysis (4ºC, maximum storage time 48h).

2.5. Metal(loid) analysis

The concentration of Fe, Mn, Zn, Ni, Cu, Sb, Mo, Cd and Pb in the derived sample digests was analyzed by inductively coupled plasma quadrupole mass spectrometry (ICP-MS, iCAP Qc, ThermoFisher Scientific, Bremen, Germany). In order to identify possible interferences, the most abundant isotopes of each metal(loid) were measured. Indium was used as an internal standard to correct for instrumental drifts. Quality control of the analytical procedure included the determination of the recovery values of the analyzed metal(loid)s in a standard reference material (NIST SRM 1648a, "Urban particulate matter"), as well as the evaluation of the blank contribution from the filters and reagents and subsequent subtraction from the results. Detection limits (LD) of the analyzed metal(loid)s were calculated based on the European standard method "EN-UNE 14902-2006". The recovery values and detection limits (LD) of the mentioned metal(loid)s are shown in Table 2.

Bioaccessible concentrations of the studied metal(loid)s in Gamble's solution and ALF were also analyzed by ICP-MS. In contrast to the sample digests mentioned before, both SLFs contain various dissolved salts, which can cause spectral as well as non-spectral interferences (matrix effects) during ICP-MS analysis. To minimize the potential negative effects of the individual SLF constituents, a reduction of their initial concentration level is required. Thus, a study was carried out prior to sample analysis to select the minimum suitable dilution to avoid the presence of matrix effects caused by the SLFs. A 1:100 dilution was needed to determine the bioaccessible concentrations in Gamble's solution. In order to avoid the use of higher dilutions, a determination of the bioaccessible concentrations in ALF was performed by adding this fluid to the

Multielemental Standard solution used to calibrate the instrument. Gamble's solution and ALF blanks were also measured. The limits of detection (LD) of the analyzed metal(loid)s in both SLFs are shown in Table 2.

2.6. Bioaccessible fraction calculation

The percentage of metal(loid) bioaccessible fraction (BF) was calculated as follows:

$$BF(\%) = \frac{C_{bio}}{C_t} \times 100 \qquad (1)$$

where C_{bio} is the metal(loid) bioaccessible concentration in Gamble's solution or ALF (ng/m^3) and C_t is the total metal(loid) concentration determined by the total digestion procedure (ng/m^3).

2.7. Exposure assessment and inhalation risk characterization

Exposure assessment generally includes: 1) identification of potentially exposed populations; 2) identification of potential pathways and conditions of exposure; 3) quantification of potential doses or chemical intake (US EPA, 2003a). In this work, three groups of population were considered to be differently exposed to metal(loid)s associated with PM_{10} in the study area: I) Residents, including children and older people; II) residents, but working outside the studied area; III) workers (not living in the area). Scenarios I and III were considered as example exposure scenarios in the US EPA (2009); scenario II was considered as an intermediate exposure. Based on the supplemental guidance for inhalation risk assessment (part F) (US EPA, 2009) inhalation exposure concentrations for each metal(loid) (EC_i) were calculated as follows:

$$EC_i = C_i \times \frac{ET \times EF \times ED}{AT} \qquad (2)$$

where C_i is the metal(loid) concentration (µg/m^3); ET is the exposure time (hours/day); EF is the exposure frequency (days/year); ED is the exposure duration (years); AT is the average time (AT = ED x 365 days x 24 hours/day for non-carcinogenic and AT = 70 x 365 days x 24 hours/day for carcinogenic risk assessments). The metal(loid) concentration used in equation (1) was based on: a) total metal(loid) content; b) bioaccessible metal(loid) concentration in Gamble's solution; c) bioaccessible

metal(loid) concentration in ALF. Ideally, C_i should be the true average concentration within the exposure unit, however, because of the uncertainty associated with the average concentration estimated at a site, the 95 percent upper confidence limit (UCL) of the arithmetic mean was used as a conservative estimate of the mean concentration (US EPA, 2007).

Table 3 shows the exposure factors used in this study for the calculation of EC_i. Factors for scenarios I and III were taken from recommended default exposure factors given in US EPA (2014).

The health risk assessment was performed separately for non-carcinogenic and carcinogenic effects. Among the trace elements considered in the present study, Ni, Mn and Cd are included in the Regional Screening Levels for Chemical Contaminants at Superfund Sites (US EPA, 2017) for non-carcinogenic risk, and Ni and Cd for carcinogenic risk. Therefore, these trace metals are considered in the inhalation risk calculation. The non-carcinogenic and carcinogenic risks for the selected metal(loid)s were determined by their hazard quotient (HQ_i) and carcinogenic risk (CR_i), respectively. The HQ_i and CR_i were calculated using the following equations:

$$HQ_i = \frac{EC_i}{RfC_i \times 1000\ \mu g\ mg^{-1}} \qquad (3)$$

$$CR_i = IUR_i \times EC_i \qquad (4)$$

where RfC_i is the reference concentration for chronic inhalation exposure for a given metal(loid) ($mg \cdot m^{-3}$) and IUR_i is its inhalation unit risk ($(\mu g \cdot m^{-3})^{-1}$. The RfC_i and IUR_i of each metal(loid) were obtained, if available, from the Integrated Risk Information System (IRIS). The US EPA has established a reference concentration (RfC) for Mn, but not for Cd and Ni. RfC equivalent levels for Cd and Ni are given in US EPA (2017) in agreement with the hierarchy of human health toxicity values used by the institution when performing human health risk assessments (US EPA, 2003b); in particular, the RfC equivalent value for Cd was obtained from ATSDR (chronic-duration inhalation minimal risk level, MRL), and the RfC equivalent value for Ni from the California EPA (chronic inhalation reference exposure level (REL), for nickel compounds). Table 4 shows the toxicity reference values (i.e. RfC_i, MRL_i and REL_i) and IUR_i used in this study. An HQ_i higher than one is considered to be an indicator of adverse health effects for the exposed population, whereas CR_i, 1.0×10^{-6} is used as the threshold lifetime cancer risk (US EPA, 1994). However, when the cancer risk is within the range of 1.0 x

10^{-6} to 1.0 x 10^{-4}, a decision about whether or not to take action is a site-specific determination (US EPA, 1994).

The hazard index (HI) is then calculated as the sum of the individual HQi for non-carcinogenic elements, or CRi for carcinogenic elements.

$$HI_{nc} = \sum HQ_i \quad (5)$$

$$HI_c = \sum CR_i \quad (6)$$

2.8 Data analysis

Statistical analysis of the data was performed using R statistical software version 3.3.0. All data distributions were checked for normality using the Shapiro-Wilks test. This test was selected due to the small size of the dataset. Since most distributions deviated from the normality, the relationship between total metal(loid) concentrations at each studied site was evaluated by determining of the Spearman correlation coefficients. The statistical significance between the mean metal(loid) bioaccessible fractions at the ETSIIT and Vidriera sites was evaluated by the parametric t-Student test for normally distributed data and by the non-parametric Mann-Whitney test when the data distributions deviated from the normality. A probability level of $p < 0.05$ was chosen to establish statistical significance.

3. Results and discussion

3.1. Total metal(loid) content

The minimum, maximum, mean, median and standard deviation of total metal(loid) concentrations associated with PM_{10} at the ETSIIT and Vidriera sites are summarized in Table 5. Metal(loid) concentrations in PM_{10} were higher at the Vidriera site with respect to the ETSIIT site in accordance with its greater proximity to industrial metal(loid) sources (mainly the ferromanganese alloy plant). As Table 5 shows, mean values of Ni, Cd and Pb are 0.6, 0.3 and 15.3 ng/m^3 at the ETSIIT site and 1.4, 2.8 and 44.6 ng/m^3 at the Vidriera site. Although these mean values correspond to a relatively short period (20 consecutive days), the annual mean is expected to be below the annual target/limit values established by Directive 2004/107/EC for Ni and Cd (20 and 5 ng/m^3, respectively) and by Directive 2008/50/EC for Pb (500 ng/m^3). Despite the fact that Mn is not regulated by EU air quality Directives, the World Health Organization (WHO)

recommends an annual mean value of 150 ng/m^3 as a guideline, in accordance with the reported association between Mn exposure and negative health effects, primarily neurotoxic disorders (Chen et al., 2016; Lucchini et al., 2012). As Table 5 shows, the mean Mn level in the air at the Vidriera site was 901.1 ng/m^3, which is similar to the annual mean measured near this site in 2009, 1072 ng/m^3 (CIMA, 2010). This suggests that the WHO's recommendation for Mn will be exceeded by far in 2017 at the Vidriera site. Also, the maximum daily concentration reached 2688 ng/m^3 at this location. Mn levels at the ETSIIT site were much lower (mean value of 74.6 ng/m^3).

The Spearman correlation coefficients between the analyzed metal(loid)s were evaluated. Correlation matrices calculated at the ETSIIT and Vidriera sites are presented in Table 6 and Table 7, respectively. At the Vidriera site Mn-Fe, Mn-Zn, Mn-Cd, Mn-Pb, Zn-Pb, Zn-Cd, Cd-Pb and Cu-Sb presented the strongest Spearman correlation coefficients ($r > 0.8$, $p < 0.01$), therefore suggesting the presence of common sources for these highly correlated metal(loid)s. Lower, but still significant correlation coefficients were found for Fe-Ni, Fe-Zn, Fe-Mo, Fe-Cd, Fe-Pb, Ni-Mo and Sb-Pb. A recent study carried out in the southern part of Santander Bay by this research group identified the presence of the ferromanganese alloy plant as the main source of metal(loid)s in the air (mainly Mn, Fe, Zn, Cd and Pb), followed by vehicular traffic (main tracers being Cu, Fe and Sb) and to a minor extent oil combustion processes (main tracers Ni, As and V) (Hernández-Pellón and Fernández-Olmo, 2017).

The correlation coefficients at the ETSIIT site are much lower than those calculated at the Vidriera site; only Zn-Cd were strongly correlated ($r > 0.8$, $p < 0.01$), whereas Fe-Zn, Fe-Cd, Fe-Pb and Cu-Pb presented lower but still significant correlation coefficients. The difference between the correlation matrices of both locations could be explained because of their different distances from the industrial sources. While the Vidriera site is mainly influenced by the presence of the ferroalloy plant, the metal(loid) levels in the air at the ETSIIT site could be attributed to several distant industrial sources (i.e. a steel plant and a ferromanganese plant) together with other urban metal(loid)s sources (road traffic, domestic heating, etc).

3.2. Bioaccessibility of metal(loid)s by extraction in SLFs

The bioaccessibility of metal(loid)s associated with PM_{10} in Gamble's solution and ALF is presented in Figures 1 and 2, respectively. Boxplots show the bioaccessible fractions of the metal(loid)s as the relative percentage of their total content in samples.

At the Vidriera site the average metal(loid) bioaccessibility in Gamble's solution followed the order Sb (47.3%) > Zn (45.5%) > Cd (39.3%) > Mn (34.1%) > Cu (18.8%) > Pb (14.8%) > Fe (4.0%). Comparable solubility in Gamble's solution was reported by Mbengue et al. (2015) in $PM_{2.5}$ samples collected 800 m from a FeMn smelter for Fe, Mn, Zn, Cd and Pb. Mean bioaccessible fractions in ALF were Mn (89.0%) > Pb (87.5%) > Cu (75.4%) > Cd (74.5%) > Sb (72.1%) > Mo (71.4%) > Zn (66.8%) > Fe (23.4%). As can be observed, all the metal(loid)s were more soluble in ALF mainly due to the greater acidity of this fluid (Pelfrêne et al., 2017; Wiseman and Zereini, 2014) and its complexation capacity. In this regard, Hedberg et al. (2011) found that the extent of metal release from stainless steel powders (sized <45 μm and <4 μm) was mainly controlled by the complexation capacity of some components present in ALF. These authors reported that ligand-induced metal release was most important for Fe, followed by Ni and to a lesser extent for Mn.

At the ETSIIT site average bioaccessible fractions were Mn (23.0%) > Cd (22.0%) > Zn (18.5%) > Pb (11.4%) > Cu (9.3%) > Fe (1.3%) in Gamble's solution and Pb (77.6%) > Mn (75.4%) > Sb (68.6%) > Cd (65.1%) > Cu (45.1%) > Zn (43.8%) > Fe (12.2%) in ALF. Similar Mn solubility in Gamble's solution (on average 27%) was found by Wiseman and Zereini (2014) in PM_{10} samples collected from an urban area mainly influenced by traffic, whereas mean values of Pb (26%) and also Mn and Pb solubility in ALF (on average 57% and 96%, respectively) showed some deviations with respect to the present study. Comparable results have also been reported in urban areas by Mukhtar et al. (2015) for Pb and Zn in Graz (Austria) and for Cd and Mn in Karachi (Pakistan). Bioaccessibility results obtained for Cu at both the ETSIIT and Vidriera sites were in general lower than those found in other urban and industrial areas (Mbengue et al., 2015; Wiseman and Zereini, 2014). The only similar values were reported by Mukhtar et al. (2015) in Graz (Austria). Bioaccessibility fractions of Ni in both SLFs, Sb in Gamble's solution at ETSIIT site and Mo in Gamble's solution in both locations and in ALF at ETSIIT site are not presented in Figures 1 and 2 due to the large number of samples below the detection limit.

As Figures 1 and 2 show, most of the analyzed metal(loid)s had moderate bioaccessibility in Gamble's solution and high bioaccessibility in ALF; only Fe had low solubilities in both SLFs, with a significant variability between samples. This variability could be explained by the different contribution from metal(loid) emission sources, which depends on both meteorological conditions (i.e. wind speed and direction and

precipitation) and emission patterns from the different anthropogenic activities, occurring during the sampling period. At the Vidriera site, this variability is attributed to the variety of point and fugitive emission sources inside the ferromanganese alloy plant (Davourie et al., 2017), which may lead to the emission of particles with different physicochemical characteristics (Hernández-Pellón et al., 2017). In this regard, a previous study carried out in this area reported that fugitive emissions from the ferromanganese alloy plant accounted for 72% of the total Mn emissions (66% from furnace buildings and 6% from ore/slag piles), whereas up to 30% of the point source emissions were produced by non-systematic sources and released without any treatment. In addition, it was also verified that bioaccessibility of all the analyzed metal(loid)s in both SLFs is significantly higher on average at the Vidriera site, which is closer to the industrial metal(loid) sources. This general decrease of the bioaccessibility with distance from the industrial sources was also reported by Mbengue et al. (2015) for Cd, Mn, Pb, Zn and Cu in PM_1 samples collected from an urban area located close to metallurgical activities and could be attributed to the mixture of metal(loid)s from different origins during transport between the industrial zone and the urban area (Mbengue et al., 2015). The greater solubility found at the Vidriera site with respect to the ETSIIT site may lead to a greater potential hazard to human health within the proximities of the industrial activities. In this regard, Mn is a metal of special concern, since it is present in the air at high concentrations and due to its moderate/high solubility in Gamble's solution and ALF, respectively. Additionally, a previous study showed that most particles observed in PM_{10} samples collected at the Vidriera site contained Mn, and were mostly characterized by spherical shapes and small sizes, with most of them in the submicron range, known to be the most harmful to health (Hernández-Pellón et al., 2017). Although Mn^0 and Mn^{2+} are the predominant oxidation states found in the inhalable aerosol fraction in FeMn and SiMn plants, Mn^{3+} and Mn^{4+} have also been previously identified in the literature (Thomassen et al., 2001). The coexistence of several Mn compounds with different oxidation states and solubilities in the vicinities of manganese alloy plants might explain the remarkable variability found in Mn bioaccessible fractions between samples.

3.3. Health risk assessment

The non-carcinogenic risk associated with Mn, Ni and Cd exposure via the inhalation route at the ETSIIT and Vidriera sites is shown in Table 8. The risk associated with Ni and Cd was considered acceptable at both sites (HQ <1). Only the HQs calculated for Mn were above the safe limit value (HQ>1), representing in all cases more than 95% of the calculated hazard index (HI). At the ETSIIT site, risk assessments based on Mn total content and on its soluble fraction in ALF showed potentially adverse health effects for residents working in the urban site as well as for those residing but not working there (Scenario I and II, respectively). Risk assessment based on the soluble fraction in Gamble's solution and risk associated with scenario III for both Mn total content and soluble fractions in SLFs were found to be acceptable (HQ<1). At the Vidriera site, all HQ's calculated for Mn were above the safe limit value. The worst-case exposure scenario (Scenario I) led to a very high HQ (24.7) when its calculation was based on the traditional approach (C_{Mn} based on total content). A HQ of 2.21 was obtained when the best-case scenario was applied (Scenario III and C_{Mn} based on soluble fraction in Gamble's solution). As Table 8 shows, the non-carcinogenic risk associated with Mn exposure is above the safe limit value (HQ>1) under most scenarios, indicating a high chronic health risk at the studied sites, especially at the Vidriera site. Although this analysis is derived from a short sampling campaign, similar Mn annual mean levels (781 ng/m^3 and 1072 ng/m^3) were measured at the Vidriera site in 2005 and 2009 respectively (CIMA, 2006; CIMA, 2010). Therefore, although caution should be taken when interpreting these results, the calculated risk for Mn is assumed to be representative of a chronic exposure.

Recent studies focused on the effects of chronic Mn exposure in the overall population suggest that Mn environmental exposure can cause neurobehavioral effects (Zoni et al., 2007). These effects may vary from tremor and motor dysfunctions (Bowler et al., 2012; Bowler et al., 2016; Rodríguez-Agudelo et al., 2006) to cognitive deficits (Bowler et al., 2015) in both adults and children (Lucchini et al., 2012; Menezes-Filho et al., 2011; Rodríguez-Barranco et al., 2013).

As was discussed in the introduction section, the risk calculation based on the total metal(loid) content may be overestimated; however, in the case of Mn, when the exposure assessment is based on its bioaccessible concentration in the least soluble fluid (i.e. Gamble's solution) and the USEPA RfC is used to calculate the risk, this risk might actually be underestimated, since this RfC is based on total metal(loid) content. The RfC for Mn was derived from an occupational study carried out by Roels et al. (1992)

on dust collected by personal samplers; in that study, the total Mn content in respirable dust was associated with the neurofunctional performance of workers; from that study, the USEPA calculated the RfC assuming several uncertainty factors. Further works should be carried out to derive a new RfC for Mn based on the bioaccessible concentration, thereby calculating a more accurate inhalation risk. Then, an intermediate risk between that based on total metal(loid) content and on the least soluble fluid can be expected for each exposure scenario.

Carcinogenic risk via the inhalation route was evaluated at the ETSIIT and Vidriera sites for Ni and Cd, which are both considered to be carcinogenic to humans (group 1) (IARC, 2012a; IARC, 2012b). As Table 9 shows, the carcinogenic risk levels of Ni and Cd at the ETSIIT site were lower than the threshold lifetime cancer risk (CR $<1.0 \times 10^{-6}$) with a maximum HI of 3.28×10^{-7} for the most conservative approach (Scenario I, C_i based on total content). In addition, as can be seen in Table 9, no carcinogenic risk was found for Ni at the Vidriera site. On the other hand, the cancer risk associated with Cd exposure was slightly higher than the threshold lifetime cancer risk: 1.89×10^{-6} and 1.47×10^{-6} (Scenario I, C_i based on total content and on the soluble fraction in ALF, respectively), suggesting a potential carcinogenic risk for the population living close to the Vidriera site. In addition, a hazard index of 1.0×10^{-6} was determined for residents working outside the area of study (Scenario II), even though the individual CRs of Ni and Cd were below the acceptable threshold cancer risk. Although the calculated cancer risk is above the target risk (1.0×10^{-6}) under some specific scenarios at the Vidriera site, according to US EPA (1994) a cancer risk within the range of 1.0×10^{-6} to 1.0×10^{-4} implies that the decision whether or not to apply corrective measures is a site-specific determination. In addition, since the estimation of Cd exposure concentration was made based on a relatively short campaign, caution should be exercised when interpreting these results. Only a few studies report Cd values in the vicinity of ferromanganese alloy plants; for example, similar mean Cd levels (i.e. 2.2 ± 1.6 ng/m^3) were reported by Mbengue et al. (2015) from a short sampling campaign in $PM_{2.5}$ samples collected 800 m from a ferromanganese alloy plant when the plume sourcing from the plant was directed towards the sampling point. However, long-term averages and seasonal effects for Cd were not assessed near the studied ferroalloy plant, and should therefore be investigated further.

This sampling campaign was performed during the cold season (January-March 2017), when the prevailing winds come from the S/SW direction. When this wind direction is blowing, the plume sourcing from the ferroalloy plant is directed towards the NE, which may result in higher PM_{10}-metal(loid) concentrations in sites located to the N/NE of the plant, especially in the Vidriera site, which is located only 350 m north of the plant. During the warm season, the prevailing winds are S/SE and NE, which may result in a higher dispersion of the pollutants sourcing from the ferromanganese alloy plant. In this regard, the development of a new sampling campaign at the Vidriera site with a longer time span to evaluate seasonal effects would be advisable to further investigate the potential risk related to Cd exposure at this location.

4. Conclusions

Bioaccessibility in SLFs of all the analyzed metal(loid)s showed a significant variability between samples. Most of the metal(loid)s showed moderate and high bioaccessibility in Gamble's solution and ALF, respectively. Only Fe had very low solubility in Gamble's solution. The highest bioaccessible fractions were obtained with ALF at both sampling locations. Solubility of all the analyzed metal(loid)s in both SLFs was found to be higher on average at the industrial site, which suggests a greater potential hazard to human health in the vicinity of the ferromanganese alloy plant.

In accordance with this, the performed inhalation risk assessment suggested an important non-carcinogenic risk related to Mn exposure at the industrial site for the three studied scenarios. Moreover, an unacceptable risk (HQ>1) was found under specific exposure scenarios at the urban site, located 7 km from the Mn alloy plant. Therefore, the non-carcinogenic risk associated with Mn exposure should be considered in the study area, especially in the urban areas located within the proximities of the ferromanganese alloy plant. In addition, a carcinogenic risk within the range between 1.0×10^{-6} to 1.0×10^{-4} (uncertainty range), was found for Cd at the industrial location under some specific exposure scenarios. Further sampling campaigns with a longer time span (i.e. including the influence of seasonal effects on the health risk assessment) ought to be done in order to evaluate the potential risk associated with Cd exposure in the vicinities of the ferroalloy plant.

In conclusion, the results reported in this work highlight the necessity of better assessing the potentially hazardous effects to human health from metal(loid) exposure in the proximity of industrial sources. In this regard, the further study of metal(loid)

bioaccessibility in SLFs and its application to the estimation of exposure concentration and risk assessment is recommended.

Acknowledgements

This work was financially supported by the Spanish Ministry of Economy and Competitiveness (MINECO) through the CTM2013-43904R Project. Ana Hernández-Pellón would like to thank the Ministry of Economy and Competitiveness (MINECO) for the FPI and research stay grants awarded, reference numbers BES-2014-068790 and EEBB-I-17-12031.

Declaration of interest

None

References

Arruti, A., Fernández-Olmo, I., Irabien, A., 2011. Regional evaluation of particulate matter composition in an Atlantic coastal area (Cantabria region, northern Spain): Spatial variations in different urban and rural environments. Atmos. Res. 101, 280–293. doi:10.1016/j.atmosres.2011.03.001

Boisa, N., Elom, N., Dean, J.R., Deary, M.E., Bird, G., Entwistle, J.A., 2014. Development and application of an inhalation bioaccessibility method (IBM) for lead in the PM10 size fraction of soil. Environ. Int. 70, 132–142. doi:10.1016/j.envint.2014.05.021

Bowler, R. M., Beseler, C. L., Gocheva, V. V., Colledge, M., Kornblith, E. S., Julian, J. R., Y. Kim, G. Bollweg, Lobdell, D. T., 2016. Environmental exposure to manganese in air: Associations with tremor and motor function. Science of the Total Environment, 541, 646-654. 10.1016/j.scitotenv.2015.09.084

Bowler, R. M., Kornblith, E. S., Gocheva, V. V., Colledge, M. A., Bollweg, G., Kim, Y., Beseler, C., Wright, C.W., Adams, S.W., Lobdell, D. T., 2015. Environmental exposure to manganese in air: Associations with cognitive functions.Neurotoxicology, 49, 139-148. 10.1016/j.neuro.2015.06.004

Bowler, R. M., Harris, M., Gocheva, V., Wilson, K., Kim, Y., Davis, S. I., Bollweg G., Lobdell D.T., L. Ngo, Roels, H. A. , 2012. Anxiety affecting parkinsonian outcome and motor efficiency in adults of an ohio community with environmental airborne manganese exposure. International Journal of Hygiene and Environmental Health, 215(3), 393-405. 10.1016/j.ijheh.2011.10.005

Brook, R.D., Rajagopalan, S., Pope, C.A., Brook, J.R., Bhatnagar, A., Diez-Roux, A. V., Holguin, F., Hong, Y., Luepker, R. V., Mittleman, M.A., Peters, A., Siscovick, D., Smith, S.C., Whitsel, L., Kaufman, J.D., 2010. Particulate matter air pollution and cardiovascular disease: An update to the scientific statement from the american heart association. Circulation 121, 2331–2378. doi:10.1161/CIR.0b013e3181dbece1

Caboche, J., Esperanza, P., Bruno, M., Alleman, L.Y., 2011. Development of an in vitro method to estimate lung bioaccessibility of metals from atmospheric particles. J. Environ. Monit. 13, 621–630. doi:10.1039/c0em00439a

Carré, J., Gatimel, N., Moreau, J., Parinaud, J., Léandri, R., 2017. Does air pollution play a role in infertility?: a systematic review. Environ. Heal. 16, 82. doi:10.1186/s12940-017-0291-8

Chen, B., Stein, A.F., Castell, N., de la Rosa, J.D., Sanchez de la Campa, A.M., Gonzalez-Castanedo, Y., Draxler, R.R., 2012. Modeling and surface observations of arsenic dispersion from a large Cu-smelter in southwestern Europe. Atmos. Environ. 49, 114–122. doi:10.1016/j.atmosenv.2011.12.014

Chen, P., Culbreth, M., Aschner, M., 2016. Exposure, epidemiology, and mechanism of the environmental toxicant manganese. Environ. Sci. Pollut. Res. 23, 13802–13810. doi:10.1007/s11356-016-6687-0

CIMA. Government of Cantabria, 2010. Air quality evaluation and metal analysis from PM_{10} samples in Alto Maliaño. . Internal report C-077/2008.

CIMA. Government of Cantabria, 2006. Evaluation of the influence of wind direction on manganese content of PM_{10} collected in Alto de Maliaño. Internal report C-098/2004.4.

Colombo, C., Monhemius, A.J., Plant, J.A., 2008. Platinum, palladium and rhodium release from vehicle exhaust catalysts and road dust exposed to simulated lung fluids. Ecotoxicol. Environ. Saf. 71, 722–730. doi:10.1016/j.ecoenv.2007.11.011

Coufalík, P., Mikuška, P., Matoušek, T., Večeřa, Z., 2016. Determination of the bioaccessible fraction of metals in urban aerosol using simulated lung fluids. Atmos. Environ. 140, 469–475. doi:10.1016/j.atmosenv.2016.06.031

da Silva, L.I.D., Yokoyama, L., Maia, L.B., Monteiro, M.I.C., Pontes, F.V.M., Carneiro, M.C., Neto, A.A., 2015. Evaluation of bioaccessible heavy metal fractions in PM10 from the metropolitan region of Rio de Janeiro city, Brazil, using a simulated lung fluid. Microchem. J. 118, 266–271. doi:10.1016/j.microc.2014.08.004

Davourie, J., Westfall, L., Ali, M., McGough, D., 2017. Evaluation of particulate matter emissions from manganese alloy production using life-cycle assessment. Neurotoxicology 58, 180–186. doi:10.1016/j.neuro.2016.09.015

Fiordelisi, A., Piscitelli, P., Trimarco, B., Coscioni, E., Iaccarino, G., Sorriento, D., 2017. The mechanisms of air pollution and particulate matter in cardiovascular diseases. Heart Fail. Rev. 22, 337–347. doi:10.1007/s10741-017-9606-7

Guney, M., Chapuis, R.P., Zagury, G.J., 2016. Lung bioaccessibility of contaminants in particulate matter of geological origin. Environ. Sci. Pollut. Res. 23, 24422–24434. doi:10.1007/s11356-016-6623-3

Haynes, E.N., Heckel, P., Ryan, P., Roda, S., Leung, Y.K., Sebastian, K., Succop, P., 2010. Environmental manganese exposure in residents living near a ferromanganese refinery in Southeast Ohio: A pilot study. Neurotoxicology 31, 468–474. doi:10.1016/j.neuro.2009.10.011

Heal, M.R., Hibbs, L.R., Agius, R.M., Beverland, I.J., 2005. Total and water-soluble trace metal content of urban background PM 10, PM2.5 and black smoke in Edinburgh, UK. Atmos. Environ. 39, 1417–1430. doi:10.1016/j.atmosenv.2004.11.026

Hedberg, Y., Hedberg, J., Liu, Y., Wallinder, I. O., 2011. Complexation- and ligand-induced metal release from 316L particles: Importance of particle size and crystallographic structure. BioMetals, 24(6), 1099-1114. 10.1007/s10534-011-9469-7

Henderson, R.G., Verougstraete, V., Anderson, K., Arbildua, J.J., Brock, T.O., Brouwers, T., Cappellini, D., Delbeke, K., Herting, G., Hixon, G., Odnevall Wallinder, I., Rodriguez, P.H., Van Assche, F., Wilrich, P., Oller, A.R., 2014. Inter-laboratory

validation of bioaccessibility testing for metals. Regul. Toxicol. Pharmacol. 70, 170–181. doi:10.1016/j.yrtph.2014.06.021

Hernández-Pellón, A., Fernández-Olmo, I., Ledoux, F., Courcot, L., Courcot, D., 2017. Characterization of manganese-bearing particles in the vicinities of a manganese alloy plant. Chemosphere 175, 411–424. doi:10.1016/j.chemosphere.2017.02.056

Hernández-Pellón, I. Fernández-Olmo, 2017. Source identification of PM10-bound heavy metals from multi-site data near an industrialized area. 10th World Congress of Chemical Engineering (WCCE 2017), Barcelona, Spain. Congress Proceedings 1574. ISBN:978-84697-8629-1

Hleis, D., Fernández-Olmo, I., Ledoux, F., Kfoury, A., Courcot, L., Desmonts, T., Courcot, D., 2013. Chemical profile identification of fugitive and confined particle emissions from an integrated iron and steelmaking plant. J. Hazard. Mater. 250–251, 246–255. doi:10.1016/j.jhazmat.2013.01.080

Hoek, G., Krishnan, R.M., Beelen, R., Peters, A., Ostro, B., Brunekreef, B., Kaufman, J.D., 2013. Long-term air pollution exposure and cardio- respiratory mortality: a review. Environ. Heal. 12, 43. doi:10.1186/1476-069X-12-43

Huang, H., Jiang, Y., Xu, X., Cao, X., 2018. In vitro bioaccessibility and health risk assessment of heavy metals in atmospheric particulate matters from three different functional areas of Shanghai, China. Sci. Total Environ. 610–611, 546–554. doi:10.1016/j.scitotenv.2017.08.074

Huang, M., Wang, W., Chan, C.Y., Cheung, K.C., Man, Y.B., Wang, X., Wong, M.H., 2014. Contamination and risk assessment (based on bioaccessibility via ingestion and inhalation) of metal(loid)s in outdoor and indoor particles from urban centers of Guangzhou, China. Sci. Total Environ. 479–480, 117–124. doi:10.1016/j.scitotenv.2014.01.115

Huang, X., Betha, R., Tan, L.Y., Balasubramanian, R., 2016. Risk assessment of bioaccessible trace elements in smoke haze aerosols versus urban aerosols using simulated lung fluids. Atmos. Environ. 125, 505–511. doi: 10.1016/j.atmosenv.2015.06.034

International Agency for Research on Cancer (IARC), 2012a. IARC Monographs on the Evaluation of Carcinogenic Risks to Humans. Nickel and nickel compounds. Volume 100C.

International Agency for Research on Cancer (IARC), 2012b. IARC Monographs on the Evaluation of Carcinogenic Risks to Humans. Cadmium and cadmium compounds. Volume 100C.

Karanasiou, A.A., Thomaidis, N.S., Eleftheriadis, K., Siskos, P.A., 2005. Comparative study of pretreatment methods for the determination of metals in atmospheric aerosol by electrothermal atomic absorption spectrometry. Talanta 65, 1196–1202. doi:10.1016/j.talanta.2004.08.044

Kastury, F., Smith, E., Juhasz, A.L., 2017. Science of the Total Environment A critical review of approaches and limitations of inhalation bioavailability and bioaccessibility of metal (loid)s from ambient particulate matter or dust. Sci. Total Environ. 574, 1054–1074. doi:10.1016/j.scitotenv.2016.09.056

Kelly, F.J., Fussell, J.C., 2012. Size, source and chemical composition as determinants of toxicity attributable to ambient particulate matter. Atmos. Environ. 60, 504–526. doi:10.1016/j.atmosenv.2012.06.039

Lucas, E.L., Bertrand, P., Guazzetti, S., Donna, F., Peli, M., Jursa, T.P., Lucchini, R., Smith, D.R., 2015. Impact of ferromanganese alloy plants on household dust manganese levels: Implications for childhood exposure. Environ. Res. 138, 279–290. doi:10.1016/j.envres.2015.01.019

Lucchini, R.G., Guazzetti, S., Zoni, S., Donna, F., Peter, S., Zacco, A., Salmistraro, M., Bontempi, E., Zimmerman, N.J., Smith, D.R., 2012. Tremor, olfactory and motor changes in Italian adolescents exposed to historical ferro-manganese emission. Neurotoxicology 33, 687–696. doi:10.1016/j.neuro.2012.01.005

MacIntosh, D.L., Stewart, J.H., Myatt, T.A., Sabato, J.E., Flowers, G.C., Brown, K.W., Hlinka, D.J., Sullivan, D.A., 2010. Use of CALPUFF for exposure assessment in a near-field, complex terrain setting. Atmos. Environ. 44, 262–270. doi: 10.1016/j.atmosenv.2009.09.023

Majestic, B.J., Schauer, J.J., Shafer, M.M., 2007. Development of a manganese speciation method for atmospheric aerosols in biologically and environmentally relevant fluids. Aerosol Sci. Technol. 41, 925–933. doi:10.1080/02786820701564657

Mbengue, S., Alleman, L. Y., Flament, P., 2015. Bioaccessibility of trace elements in fine and ultrafine atmospheric particles in an industrial environment. Environmental Geochemistry and Health, 37(5), 875-889. doi:10.1007/s10653-015-9756-2

Menezes-Filho, J.A., Souza, K.O.F. de, Rodrigues, J.L.G., Santos, N.R. dos, Bandeira, M. de J., Koin, N.L., Oliveira, S.S. d. P., Godoy, A.L.P.C., Mergler, D., 2016. Manganese and lead in dust fall accumulation in elementary schools near a ferromanganese alloy plant. Environ. Res. 148, 322–329. doi:10.1016/j.envres.2016.03.041

Menezes-Filho, J. A., Novaes, C. D. O., Moreira, J. C., Sarcinelli, P. N., Mergler, D., 2011. Elevated manganese and cognitive performance in school-aged children and their mothers. Environmental Research, 111(1), 156-163. 10.1016/j.envres.2010.09.006

Midander, K., Wallinder, I.O., Leygraf, C., 2007. In vitro studies of copper release from powder particles in synthetic biological media. Environ. Pollut. 145, 51–59. doi:10.1016/j.envpol.2006.03.041

Mugica-Álvarez, V., Figueroa-Lara, J., Romero-Romo, M., Sepúlvea-Sánchez, J., López-Moreno, T., 2012. Concentrations and properties of airborne particles in the Mexico City subway system. Atmos. Environ. 49, 284–293. doi:10.1016/j.atmosenv.2011.11.038

Mukherjee, A., Agrawal, M., 2017. World air particulate matter: sources, distribution and health effects. Environ. Chem. Lett. 15, 283–309. doi:10.1007/s10311-017-0611-9

Mukhtar, A., Limbeck, A., 2013. Recent developments in assessment of bio-accessible trace metal fractions in airborne particulate matter: A review. Anal. Chim. Acta 774, 11–25. doi:10.1016/j.aca.2013.02.008

Mukhtar, A., Mohr, V., Limbeck, A., 2015. The suitability of extraction solutions to assess bioaccessible trace metal fractions in airborne particulate matter: a comparison of common leaching agents. Environ. Sci. Pollut. Res. 22, 16620–16630. doi:10.1007/s11356-015-4789-8

Niu, J., Rasmussen, P. E., Hassan, N. M., & Vincent, R., 2010. Concentration distribution and bioaccessibility of trace elements in nano and fine urban airborne particulate matter: Influence of particle size.Water, Air, and Soil Pollution, 213(1-4), 211-225. doi:10.1007/s11270-010-0379-z

Noh, J., Sohn, J., Cho, J., Cho, S., Choi, Y.J., Kim, C., Shin, D.C., 2016. Short-term Effects of Ambient Air Pollution on Emergency Department Visits for Asthma : An Assessment of Effect Modification by Prior Allergic Disease History 329–341.

Peixoto, M.S., de Oliveira Galvão, M.F., Batistuzzo de Medeiros, S.R., 2017. Cell death pathways of particulate matter toxicity. Chemosphere 188, 32–48. doi:10.1016/j.chemosphere.2017.08.076

Pelfrêne, A., Cave, M.R., Wragg, J., Douay, F., 2017. In vitro investigations of human bioaccessibility from reference materials using simulated lung fluids. Int. J. Environ. Res. Public Health 14, 1–15. doi:10.3390/ijerph14020112

Potgieter-Vermaak, S., Rotondo, G., Novakovic, V., Rollins, S., & van Grieken, R., 2012. Component-specific toxic concerns of the inhalable fraction of urban road dust. Environmental Geochemistry and Health, 34(6), 689-696. doi:10.1007/s10653-012-9488-5

Raaschou-Nielsen, O., Andersen, Z.J., Beelen, R., Samoli, E., Stafoggia, M., Weinmayr, G., Hoffmann, B., Fischer, P., Nieuwenhuijsen, M.J., Brunekreef, B., Xun, W.W., Katsouyanni, K., Dimakopoulou, K., Sommar, J., Forsberg, B., Modig, L., Oudin, A., Oftedal, B., Schwarze, P.E., Nafstad, P., De Faire, U., Pedersen, N.L., Östenson, C.G., Fratiglioni, L., Penell, J., Korek, M., Pershagen, G., Eriksen, K.T., Sørensen, M., Tjønneland, A., Ellermann, T., Eeftens, M., Peeters, P.H., Meliefste, K., Wang, M., Bueno-de-Mesquita, B., Key, T.J., de Hoogh, K., Concin, H., Nagel, G., Vilier, A., Grioni, S., Krogh, V., Tsai, M.Y., Ricceri, F., Sacerdote, C., Galassi, C., Migliore, E., Ranzi, A., Cesaroni, G., Badaloni, C., Forastiere, F., Tamayo, I., Amiano, P., Dorronsoro, M., Trichopoulou, A., Bamia, C., Vineis, P., Hoek, G., 2013. Air pollution and lung cancer incidence in 17 European cohorts: Prospective analyses from the European Study of Cohorts for Air Pollution Effects (ESCAPE). Lancet Oncol. 14, 813–822. doi:10.1016/S1470-2045(13)70279-1

Rodríguez-Agudelo, Y., Riojas-Rodríguez, H., Ríos, C., Rosas, I., Sabido Pedraza, E., Miranda, J., Siebe C., Texcalac J.L., Santos-Burgoa, C., 2006. Motor alterations associated with exposure to manganese in the environment in mexico. Science of the Total Environment, 368(2-3), 542-556. 10.1016/j.scitotenv.2006.03.025

Rodríguez-Barranco, M., Lacasaña, M., Aguilar-Garduño, C., Alguacil, J., Gil, F., González-Alzaga, B., Rojas-García, A., 2013. Association of arsenic, cadmium and manganese exposure with neurodevelopment and behavioural disorders in children: A systematic review and meta-analysis. Science of the Total Environment, 454-455, 562-577. 10.1016/j.scitotenv.2013.03.047

Roels, H. A., Ghyselen, P., Buchet, J. P., Ceulemans, E., & Lauwerys, R. R., 1992. Assessment of the permissible exposure level to manganese in workers exposed to manganese dioxide dust. British Journal of Industrial Medicine, 49(1), 25-34

Sánchez de la Campa, M., de la Rosa, J., González-Castanedo, Y., Fernández-Camacho, R., Alastuey, Querol, X., Stein, F., Ramos, J.L., Rodríguez, S., Orellana, I.G., Nava, S., 2011. Levels and chemical composition of PM in a city near a large Cu-smelter in Spain. J. Environ. Monit. 13, 1276–87. doi:10.1039/c0em00708k

Sylvestre, A., Mizzi, A., Mathiot, S., Masson, F., Jaffrezo, J.L., Dron, J., Mesbah, B., Wortham, H., Marchand, N., 2017. Comprehensive chemical characterization of industrial PM2.5 from steel industry activities. Atmos. Environ. 152, 180–190. doi:10.1016/j.atmosenv.2016.12.032

Taj, T., Malmqvist, E., Stroh, E., Åström, D.O., Jakobsson, K., Oudin, A., 2017. Short-term associations between air pollution concentrations and respiratory health—Comparing primary health care visits, hospital admissions, and emergency department visits in a multi-municipality study. Int. J. Environ. Res. Public Health 14. doi:10.3390/ijerph14060587

Tessier, A., Campbell, P.G.C., Bisson, M., 1979. Sequential Extraction Procedure for the Speciation of Particulate Trace Metals. Anal. Chem. 51, 844–851. doi:10.1021/ac50043a017

Thomassen, Y., Ellingsen, D.G., Hetland, S., Sand, G., 2001. Chemical speciation and sequential extraction of Mn in workroom aerosols: analytical methodology and results

from a field study in Mn alloy plants. J. Environ. Monit. 3, 555–559. doi:10.1039/b104479f

U.S. Environmental Protection Agency (EPA), 2017. Regional Screening Levels for Chemical Contaminants at Superfund Sites. Available online at: https://www.epa.gov/risk/regional-screening-levels-rsls-generic-tables-november-2017

U.S. Environmental Protection Agency (EPA), 2014. Human Health Evaluation Manual, Supplemental Guidance: Update of Standard Default Exposure Factors. Office of Superfund Remediation and Technology Innovation, Assessment and Remediation Division, Washington, DC; OSWER Directive 9200.1-120. Available online at: https://www.epa.gov/risk/update-standard-default-exposure-factors

U.S. Environmental Protection Agency (EPA), 2009. Risk Assessment Guidance for Superfund, Volume I: Human Health Evaluation Manual (Part F, Supplemental Guidance for Inhalation Risk Assessment). Office of Superfund Remediation and Technology Innovation, Washington, D.C.; EPA-540-R-070-002, OSWER 9285.7-82. Available on-line at: https://www.epa.gov/risk/risk-assessment-guidance-superfund-rags-part-f

U.S. Environmental Protection Agency (EPA), 2007. Framework for metal risk assessment. Office of the Science Advisor Risk Assessment Forum, Washington, DC; EPA 120/R-07/001. Available online at: https://www.epa.gov/risk/framework-metals-risk-assessment

U.S. Environmental Protection Agency (EPA), 2003a. Example Exposure Scenarios. National Center for Environmental Assessment, Washington, DC; EPA/600/R-03/036. Available online at: http://www.epa.gov/ncea

U.S. Environmental Protection Agency (EPA), 2003b. Human Health Toxicity Values in Superfund Risk Assessments, Washington, DC; OSWER Directive 9285.7-53.

U. S. Environmental Protection Agency (EPA), 1994. Risk assessment Guidance for Superfund Volume I – Human Health Evaluation Manual (Part B, Development of Risk-based preliminary Remediation Goals., Washington, DC; EPA/540/R-92/003.

Van Den Heuvel, R., Den Hond, E., Govarts, E., Colles, A., Koppen, G., Staelens, J., Mampaey, M., Janssen, N., Schoeters, G., 2016. Identification of PM10 characteristics involved in cellular responses in human bronchial epithelial cells (Beas-2B). Environ. Res. 149, 48–56. doi:10.1016/j.envres.2016.04.029

Verma, V., Shafer, M.M., Schauer, J.J., Sioutas, C., 2010. Contribution of transition metals in the reactive oxygen species activity of PM emissions from retrofitted heavy-duty vehicles. Atmos. Environ. 44, 5165–5173. doi:10.1016/j.atmosenv.2010.08.052

Voutsa, D., Samara, C., 2002. Labile and bioaccessible fractions of heavy metals in the airborne particulate matter from urban and industrial areas. Atmos. Environ. 36, 3583–3590. doi:10.1016/S1352-2310(02)00282-0

Wang, Y., Xiong, L., Tang, M., 2017. Toxicity of inhaled particulate matter on the central nervous system: neuroinflammation, neuropsychological effects and neurodegenerative disease. J. Appl. Toxicol. 37, 644–667. doi:10.1002/jat.3451

Wiseman, C.L.S., 2015. Analytical methods for assessing metal bioaccessibility in airborne particulate matter: A scoping review. Anal. Chim. Acta 877, 9–18. doi:10.1016/j.aca.2015.01.024

Wiseman, C.L.S., Zereini, F., 2014. Characterizing metal(loid) solubility in airborne PM10, PM2.5 and PM1 in Frankfurt, Germany using simulated lung fluids. Atmos. Environ. 89, 282–289. doi:10.1016/j.atmosenv.2014.02.055

Yatkin, S., Bayram, A., 2008. Determination of major natural and anthropogenic source profiles for particulate matter and trace elements in Izmir, Turkey. Chemosphere 71, 685–696. doi:10.1016/j.chemosphere.2007.10.070

Zereini, F., Wiseman, C.L.S., Püttmann, W., 2012. In Vitro Investigations of Platinum, Palladium, and Rhodium Mobility in Urban Airborne Particulate Matter (PM10, PM2.5, and PM1) using Simulated Lung Fluids. Environ. Sci. Technol. doi:10.1021/e

Zoni, S., Albini, E., Lucchini, R., 2007. Neuropsychological testing for the assessment of manganese neurotoxicity: A review and a proposal. American Journal of Industrial Medicine, 50(11), 812-830.

FIGURE CAPTIONS

Figure 1. Bioaccessibility in Gamble's solution of different metal(loid)s from PM_{10} samples collected at the ETSIIT and Vidriera sites

Figure 2. Bioaccessibility in ALF of different metal(loid)s from PM_{10} samples collected at the ETSIIT and Vidriera sites

Figure S1. Location of the monitoring sites and the main metal(loid) sources

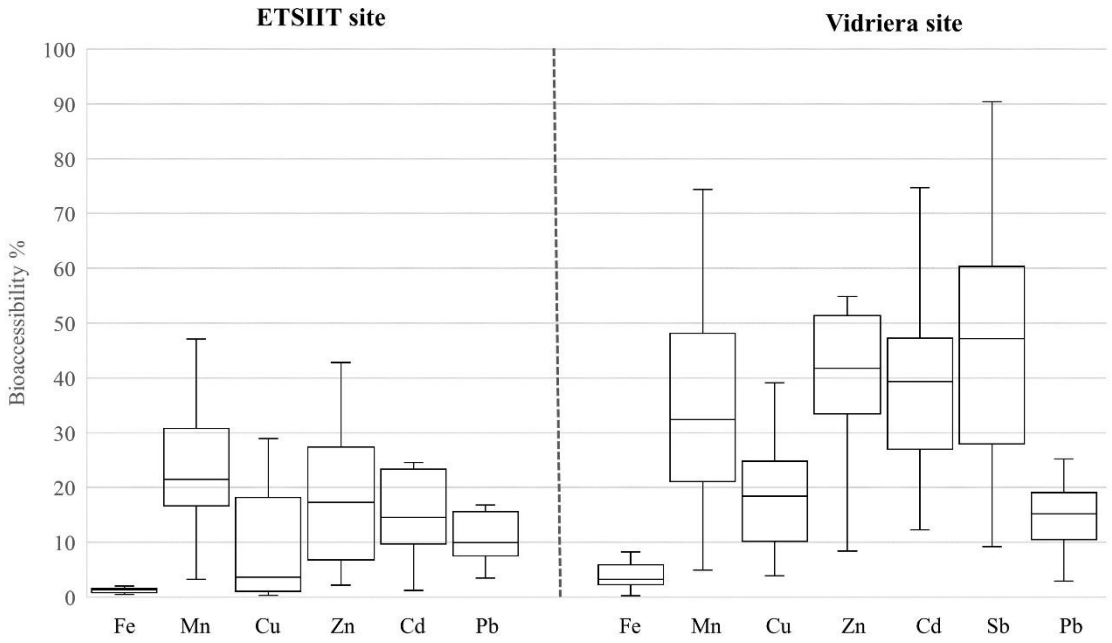

Figure 1. Bioaccessibility in Gamble's solution of different metal(loid)s from PM_{10} samples collected at the ETSIIT and Vidriera sites

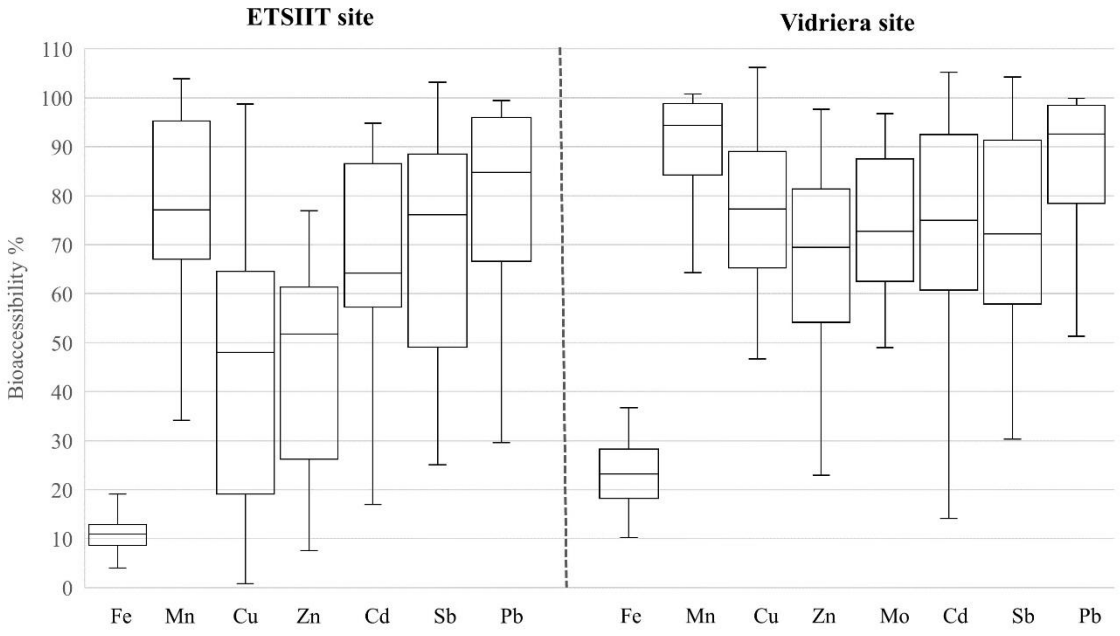

Figure 2. Bioaccessibility in ALF of different metal(loid)s from PM_{10} samples collected at the ETSIIT and Vidriera sites

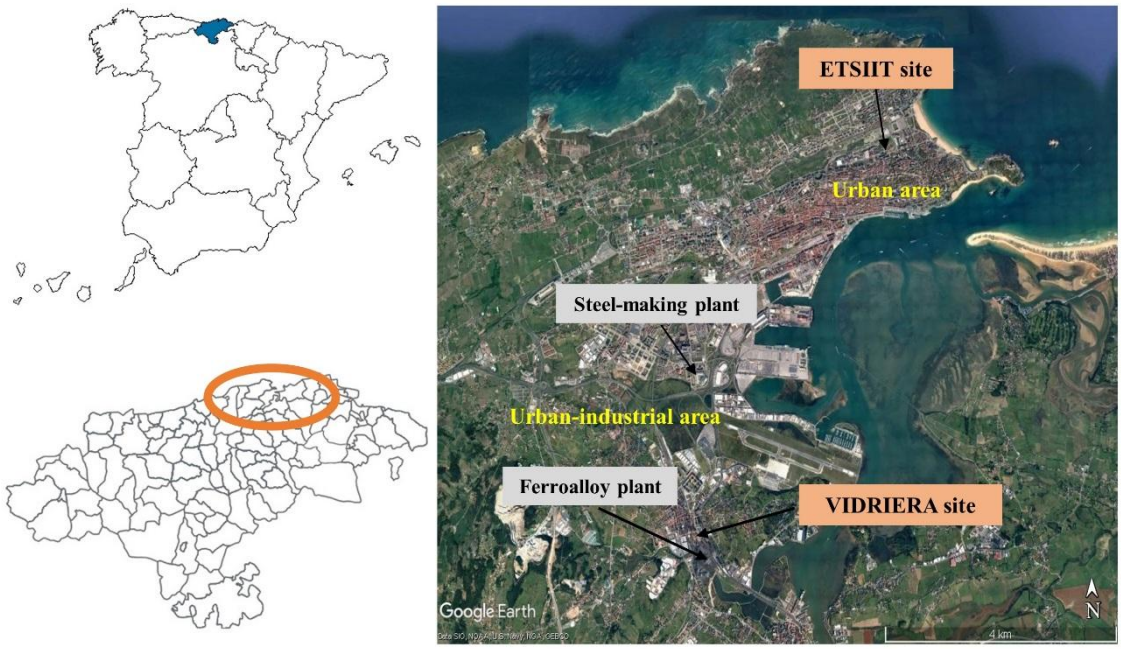

Figure S1. Location of the monitoring sites and the main metal(loid) sources

Table 1. Composition (g/L) and pH of simulated lung fluids: Gamble's solution, artificial lysosomal fluid (ALF) (Colombo et al., 2008)

Reagents	Formula	Gamble's solution (pH=7.4±0.1)	ALF (pH =4.5±0.1)
Magnesium chloride	$MgCl_2$	0.095	0.050
Sodium chloride	NaCl	6.019	3.21
Potassium chloride	KCl	0.298	-
Disodium hydrogen phosphate	Na_2HPO_4	0.126	0.071
Sodium sulphate	Na_2SO_4	0.063	0.039
Calcium chloride dihydrate	$CaCl \cdot 2H_2O$	0.368	0.128
Sodium acetate	$C_2H_3O_2Na$	0.574	-
Sodium hydrogen carbonate	$NaHCO_3$	2.604	-
Sodium citrate dihydrate	$C_6H_5Na_3O_7 \cdot 2H_2O$	0.097	0.077
Sodium hydroxide	NaOH	-	6
Citric acid	$C_6H_8O_7$	-	20.8
Glycine	NH_2CH_2COOH	-	0.059
Sodium tartrate dihydrate	$C_4H_4O_6Na_2 \cdot 2H_2O$	-	0.090
Sodium lactate	$C_3H_5NaO_3$	-	0.085
Sodium pyruvate	$C_3H_3O_3Na$	-	0.086

Table 2. Metal recovery (%) obtained for SRM 1648a and detection limits (ng/m^3) estimated for the determination of the total and bioaccessible metal(loid) content.

Element	Recovery (%)	DL (ng/m^3)	DL (ng/m^3)	DL (ng/m^3)
	SRM 1648a	Teflon filters	Gamble's solution	ALF
Mn	100.3±5.3	0.1	0.5	0.2
Fe	102.0±3.9	5.6	0.6	0.8
Ni	96.6±5.6	0.2	0.6	0.3
Cu	100.3±4.9	1.3	0.1	0.2
Zn	97.1±4.1	0.7	1.2	1.9
Mo	n.a.	0.04	0.5	0.02
Cd	85.1±2.3	0.03	0.1	0.01
Sb	83.5±1.7	0.02	0.2	0.02
Pb	102.1±5.9	0.4	0.03	0.1

n.a.: certificated value not available for the reference material (SRM 1648a)

Table 3. Environmental exposure scenarios.

Parameters	Scenario I		Scenario II	Scenario III
	Adults	Children		
ET (h/day)	24	24	12	8
EF (days/year)	350	350	350	250
ED (years)	20	6	20	25

Scenario I: Residents, including children and older people; Scenario II: Residents, but working outside the studied area; Scenario III: Workers (not living in the area)

Table 4. Parameters used in the health risk assessment.

Element	C^a (95% UCL) ng/m^3			C^b (95% UCL) ng/m^3			Toxicity reference value^{c*} mg/m^3	IUR^{d*} (µg/m^3)$^{-1}$
	Total content	Gamble	ALF	Total content	Gamble	ALF		
Mn	127.6	25.1	110.3	1286.7	484.8	1113.5	5.0×10^{-5}	-
Ni	0.9	-	-	1.8	-	-	1.4×10^{-5}	2.4×10^{-4}
Cd	0.6	0.1	0.5	3.8	1.7	3.0	1.0×10^{-5}	1.8×10^{-3}

a: 95% upper confidence limit (UCL) of the mean contents (ETSIIT site)

b: 95% upper confidence limit (UCL) of the mean contents (Vidriera site)

c: Reference concentration for chronic inhalation exposure (RfC) for Mn; chronic-duration inhalation minimal risk level (MRL) for Cd; chronic inhalation reference exposure level (REL) for Ni.

d: Inhalation unit risk (IUR)

*RfC and IUR taken from the Integrated Risk Information System (IRIS, US EPA). MRL and REL taken from the Regional Screening Levels for Chemical Contaminants at Superfund Sites (US EPA, 2017)

Table 5. Total metal(loid) content (ng/m^3) in PM_{10} at the ETSIIT and Vidriera sites.

Element	ETSIIT site[a]					Vidriera site[b]				
	Max	Min	Mean*	SD	Median	Max	Min	Mean*	SD	Median
Mn	507.0	1.3	74.6	113.2	34.5	2688.3	11.1	901.1	823.8	632.6
Fe	811.1	72.8	295.7	185.5	258.7	2091.1	127.8	691.5	470.3	543.4
Ni	1.7	<d.l.	0.6	0.5	0.4	3.4	<d.l.	1.4	0.9	1.2
Cu	39.4	<d.l.	8.2	9.5	6.2	44.3	<d.l.	18.5	13.0	12.6
Zn	314.8	3.3	77.1	73.7	56	814.9	12.3	250.5	205.3	177.1
Mo	3.7	<d.l.	0.5	1.1	0.1	6.1	<d.l.	0.8	1.4	0.4
Cd	2.0	<d.l.	0.3	0.5	0.2	6.6	0.1	2.8	2.2	2.2
Sb	2.3	<d.l.	0.4	0.5	0.3	10.4	0.2	1.7	2.4	1.0
Pb	56.6	1.2	15.3	13.7	12.3	110.4	1.8	44.6	33.6	36.5

a: February-March 2017. 20 daily samples.
b: January-February 2017. 20 daily samples.
* Arithmetic mean
<d.l. below detection limit of the method

Table 6: Spearman correlation matrix for the total metal(loid) content in PM_{10} (ng/m^3) samples collected at the ETSIIT site.

	Fe	Ni	Cu	Zn	Mo	Cd	Sb	Pb
Mn	0.386	0.052	-0.267	0.253	0.253	**0.596**	0.201	**0.451**
Fe		0.449	-0.583	**0.668**	0.305	**0.645**	**0.581**	**0.731**
Ni			-0.167	0.441	0.332	0.382	0.412	0.167
Cu				-0.417	0.512	0.429	0.150	**0.667**
Zn					0.095	**0.808**	0.160	0.390
Mo						0.136	0.463	0.042
Cd							0.095	0.471
Sb								0.386

In bold character correlation is significant at the 0.01 level.

Table 7: Spearman correlation matrix for the total metal(loid) content in PM_{10} (ng/m^3) samples collected at the Vidriera site.

	Fe	Ni	Cu	Zn	Mo	Cd	Sb	Pb
Mn	**0.808**	0.447	0.321	**0.942**	0.459	**0.896**	0.321	**0.856**
Fe		**0.732**	0.432	**0.768**	**0.698**	**0.700**	0.422	**0.738**
Ni			0.170	0.405	**0.678**	0.418	0.130	0.313
Cu				0.363	0.406	0.355	**0.825**	0.501
Zn					0.518	**0.881**	0.274	**0.926**
Mo						0.517	0.291	0.554
Cd							0.203	**0.824**
Sb								**0.495**

In bold character correlation is significant at the 0.01 level.

Table 8. Non-carcinogenic HQ and HI: ETSIIT and Vidriera sites.

Element	Site	Based on total metal content			Based on soluble metal: Gamble's solution			Based on soluble metal: ALF		
		Scenario I[a]	Scenario II[b]	Scenario III[c]	Scenario I[a]	Scenario II[b]	Scenario III[c]	Scenario I[a]	Scenario II[b]	Scenario III[c]
Mn	ETSIIT	**2.45**	**1.22**	0.58	0.48	0.24	0.11	**2.12**	**1.06**	0.50
	Vidriera	**24.7**	**12.3**	**5.87**	**9.30**	**4.64**	**2.21**	**21.4**	**10.7**	**5.08**
Ni	ETSIIT	0.06	0.03	0.01	-	-	-	-	-	-
	Vidriera	0.12	0.06	0.03	-	-	-	-	-	-
Cd	ETSIIT	0.05	0.03	0.01	0.01	0.004	0.002	0.05	0.02	0.01
	Vidriera	0.37	0.18	0.09	0.16	0.08	0.04	0.29	0.14	0.07
HI	ETSIIT	**2.56**	**1.28**	0.60	0.49	0.24	0.12	**2.16**	**1.08**	0.51
	Vidriera	**25.2**	**12.5**	**5.99**	**9.46**	**4.72**	**2.25**	**21.6**	**10.8**	**5.15**

Scenario I: Residents, including children and older people; Scenario II: Residents, but working outside the studied area; Scenario III: Workers (not living in the area)

Table 9. Carcinogenic CR and HI: ETSIIT and Vidriera sites.

Element	Site	Based on total metal content			Based on soluble metal: Gamble's solution			Based on soluble metal: ALF		
		Scenario I**	Scenario II	Scenario III	Scenario I**	Scenario II	Scenario III	Scenario I**	Scenario II	Scenario III
Ni*	ETSIIT	5.72E-08/1.71E-08	2.86E-08	1.69E-08	-	-	-	-	-	-
	Vidriera	1.17E-07/3.50E-08	5.85E-08	3.46E-08	-	-	-	-	-	-
Cd	ETSIIT	2.71E-07/8.12E-08	1.36E-07	8.02E-08	3.95E-08/1.18E-08	1.97E-08	1.17E-08	2.52E-07/7.35E-08	1.26E-07	7.44E-08
	Vidriera	**1.89E-06**/5.65E-07	9.44E-07	5.58E-07	8.29E-07/2.48E-07	4.14E-07	2.45E-07	**1.47E-06**/4.40E-07	7.35E-07	4.34E-07
HI	ETSIIT	3.28E-07/9.83E-08	1.65E-07	9.71E-08	3.95E-08/1.18E-08	1.97E-08	1.17E-08	2.52E-07/7.35E-08	1.26E-07	7.44E-08
	Vidriera	**2.0E-06**/6.0E-07	**1.0E-06**	5.93E-07	8.29E-07/2.48E-07	4.14E-07	2.45E-07	**1.47E-06**/4.40E-07	7.35E-07	4.34E-07

Scenario I: Residents, including children and older people; Scenario II: Residents, but working outside the studied area; Scenario III: Workers (not living in the area)

*Bioaccessible fractions of Ni in SLFs were not determined

** First value corresponds to adult. Second value corresponds to children

Table 1

Table 1. Composition (g/L) and pH of simulated lung fluids: Gamble's solution, artificial lysosomal fluid (ALF) (Colombo et al., 2008)

Reagents	Formula	Gamble's solution (pH=7.4±0.1)	ALF (pH =4.5±0.1)
Magnesium chloride	$MgCl_2$	0.095	0.050
Sodium chloride	NaCl	6.019	3.21
Potassium chloride	KCl	0.298	-
Disodium hydrogen phosphate	Na_2HPO_4	0.126	0.071
Sodium sulphate	Na_2SO_4	0.063	0.039
Calcium chloride dihydrate	$CaCl \cdot 2H_2O$	0.368	0.128
Sodium acetate	$C_2H_3O_2Na$	0.574	-
Sodium hydrogen carbonate	$NaHCO_3$	2.604	-
Sodium citrate dihydrate	$C_6H_5Na_3O_7 \cdot 2H_2O$	0.097	0.077
Sodium hydroxide	NaOH	-	6
Citric acid	$C_6H_8O_7$	-	20.8
Glycine	NH_2CH_2COOH	-	0.059
Sodium tartrate dihydrate	$C_4H_4O_6Na_2 \cdot 2H_2O$	-	0.090
Sodium lactate	$C_3H_5NaO_3$	-	0.085
Sodium pyruvate	$C_3H_3O_3Na$	-	0.086

Table 2

Table 2. Metal recovery (%) obtained for SRM 1648a and detection limits (ng/m^3) estimated for the determination of the total and bioaccessible metal(loid) content.

Element	Recovery (%)	DL (ng/m^3)	DL (ng/m^3)	DL (ng/m^3)
	SRM 1648a	Teflon filters	Gamble's solution	ALF
Mn	100.3±5.3	0.1	0.5	0.2
Fe	102.0±3.9	5.6	0.6	0.8
Ni	96.6±5.6	0.2	0.6	0.3
Cu	100.3±4.9	1.3	0.1	0.2
Zn	97.1±4.1	0.7	1.2	1.9
Mo	n.a.	0.04	0.5	0.02
Cd	85.1±2.3	0.03	0.1	0.01
Sb	83.5±1.7	0.02	0.2	0.02
Pb	102.1±5.9	0.4	0.03	0.1

n.a.: certificated value not available for the reference material (SRM 1648a)

Table 3

Table 3. Environmental exposure scenarios.

Parameters	Scenario I		Scenario II	Scenario III
	Adults	Children		
ET (h/day)	24	24	12	8
EF (days/year)	350	350	350	250
ED (years)	20	6	20	25

Scenario I: Residents, including children and older people; Scenario II: Residents, but working outside the studied area; Scenario III: Workers (not living in the area)

Table 4

Table 4. Parameters used in the health risk assessment.

Element	C^a (95% UCL) ng/m^3			C^b (95% UCL) ng/m^3			Toxicity reference value^{c*} mg/m^3	IUR^{d*} (µg/m^3)$^{-1}$
	Total content	Gamble	ALF	Total content	Gamble	ALF		
Mn	127.6	25.1	110.3	1286.7	484.8	1113.5	5.0×10^{-5}	-
Ni	0.9	-	-	1.8	-	-	1.4×10^{-5}	2.4×10^{-4}
Cd	0.6	0.1	0.5	3.8	1.7	3.0	1.0×10^{-5}	1.8×10^{-3}

a: 95% upper confidence limit (UCL) of the mean contents (ETSIIT site)

b: 95% upper confidence limit (UCL) of the mean contents (Vidriera site)

c: Reference concentration for chronic inhalation exposure (RfC) for Mn; chronic-duration inhalation minimal risk level (MRL) for Cd; chronic inhalation reference exposure level (REL) for Ni.

d: Inhalation unit risk (IUR)

*RfC and IUR taken from the Integrated Risk Information System (IRIS, US EPA). MRL and REL taken from the Regional Screening Levels for Chemical Contaminants at Superfund Sites (US EPA, 2017)

Table 5

Table 5. Total metal(loid) content (ng/m^3) in PM_{10} at the ETSIIT and Vidriera sites.

Element	ETSIIT site[a]					Vidriera site[b]				
	Max	Min	Mean*	SD	Median	Max	Min	Mean*	SD	Median
Mn	507.0	1.3	74.6	113.2	34.5	2688.3	11.1	901.1	823.8	632.6
Fe	811.1	72.8	295.7	185.5	258.7	2091.1	127.8	691.5	470.3	543.4
Ni	1.7	<d.l.	0.6	0.5	0.4	3.4	<d.l.	1.4	0.9	1.2
Cu	39.4	<d.l.	8.2	9.5	6.2	44.3	<d.l.	18.5	13.0	12.6
Zn	314.8	3.3	77.1	73.7	56	814.9	12.3	250.5	205.3	177.1
Mo	3.7	<d.l.	0.5	1.1	0.1	6.1	<d.l.	0.8	1.4	0.4
Cd	2.0	<d.l.	0.3	0.5	0.2	6.6	0.1	2.8	2.2	2.2
Sb	2.3	<d.l.	0.4	0.5	0.3	10.4	0.2	1.7	2.4	1.0
Pb	56.6	1.2	15.3	13.7	12.3	110.4	1.8	44.6	33.6	36.5

a: February-March 2017. 20 daily samples; b: January-February 2017. 20 daily samples.

*: Aritmethic mean

<d.l. below detection limit of the method

Table 6

Table 6. Spearman correlation matrix for the total metal(loid) content in PM_{10} (ng/m^3) samples collected at the ETSIIT site.

	Fe	Ni	Cu	Zn	Mo	Cd	Sb	Pb
Mn	0.386	0.052	-0.267	0.253	0.253	**0.596**	0.201	**0.451**
Fe		0.449	-0.583	**0.668**	0.305	**0.645**	**0.581**	**0.731**
Ni			-0.167	0.441	0.332	0.382	0.412	0.167
Cu				-0.417	0.512	0.429	0.150	**0.667**
Zn					0.095	**0.808**	0.160	0.390
Mo						0.136	0.463	0.042
Cd							0.095	0.471
Sb								0.386

In bold character correlation is significant at the 0.01 level.

Table 7

Table 7. Spearman correlation matrix for the total metal(loid) content in PM_{10} (ng/m^3) samples collected at the Vidriera site.

	Fe	Ni	Cu	Zn	Mo	Cd	Sb	Pb
Mn	**0.808**	0.447	0.321	**0.942**	0.459	**0.896**	0.321	**0.856**
Fe		**0.732**	0.432	**0.768**	**0.698**	**0.700**	0.422	**0.738**
Ni			0.170	0.405	**0.678**	0.418	0.130	0.313
Cu				0.363	0.406	0.355	**0.825**	0.501
Zn					0.518	**0.881**	0.274	**0.926**
Mo						0.517	0.291	0.554
Cd							0.203	**0.824**
Sb								**0.495**

In bold character correlation is significant at the 0.01 level.

Table 8

Table 8. Non-carcinogenic HQ and HI: ETSIIT and Vidriera sites.

Element	Site	Based on total metal content			Based on soluble metal: Gamble's solution			Based on soluble metal: ALF		
		Scenario I	Scenario II	Scenario III	Scenario I	Scenario II	Scenario III	Scenario I	Scenario II	Scenario III
Mn	ETSIIT	**2.45**	**1.22**	0.58	0.48	0.24	0.11	**2.12**	**1.06**	0.50
	Vidriera	**24.7**	**12.3**	**5.87**	**9.30**	**4.64**	**2.21**	**21.4**	**10.7**	**5.08**
Ni	ETSIIT	0.06	0.03	0.01	-	-	-	-	-	-
	Vidriera	0.12	0.06	0.03	-	-	-	-	-	-
Cd	ETSIIT	0.05	0.03	0.01	0.01	0.004	0.002	0.05	0.02	0.01
	Vidriera	0.37	0.18	0.09	0.16	0.08	0.04	0.29	0.14	0.07
HI	ETSIIT	**2.56**	**1.28**	0.60	0.49	0.24	0.12	**2.16**	**1.08**	0.51
	Vidriera	**25.2**	**12.5**	**5.99**	**9.46**	**4.72**	**2.25**	**21.6**	**10.8**	**5.15**

Scenario I: Residents, including children and older people; Scenario II: Residents, but working outside the studied area; Scenario III: Workers (not living in the area)

Table 9

Table 9. Carcinogenic CR and HI: ETSIIT and Vidriera sites.

Element	Site	Based on total metal content			Based on soluble metal: Gamble's solution			Based on soluble metal: ALF		
		Scenario I**	Scenario II	Scenario III	Scenario I**	Scenario II	Scenario III	Scenario I**	Scenario II	Scenario III
Ni*	ETSIIT	5.72E-08/1.71E-08	2.86E-08	1.69E-08	-	-	-	-	-	-
	Vidriera	1.17E-07/3.50E-08	5.85E-08	3.46E-08	-	-	-	-	-	-
Cd	ETSIIT	2.71E-07/8.12E-08	1.36E-07	8.02E-08	3.95E-08/1.18E-08	1.97E-08	1.17E-08	2.52E-07/7.35E-08	1.26E-07	7.44E-08
	Vidriera	**1.89E-06**/5.65E-07	9.44E-07	5.58E-07	8.29E-07/2.48E-07	4.14E-07	2.45E-07	**1.47E-06**/4.40E-07	7.35E-07	4.34E-07
HI	ETSIIT	3.28E-07/9.83E-08	1.65E-07	9.71E-08	3.95E-08/1.18E-08	1.97E-08	1.17E-08	2.52E-07/7.35E-08	1.26E-07	7.44E-08
	Vidriera	**2.0E-06**/6.0E-07	**1.0E-06**	5.93E-07	8.29E-07/2.48E-07	4.14E-07	2.45E-07	**1.47E-06**/4.40E-07	7.35E-07	4.34E-07

Scenario I: Residents, including children and older people; Scenario II: Residents, but working outside the studied area; Scenario III: Workers (not living in the area)

*Bioaccessible fractions of Ni in SLFs were not determined

** First value corresponds to adult. Second value corresponds to children

Figure 1

Click here to download high resolution image

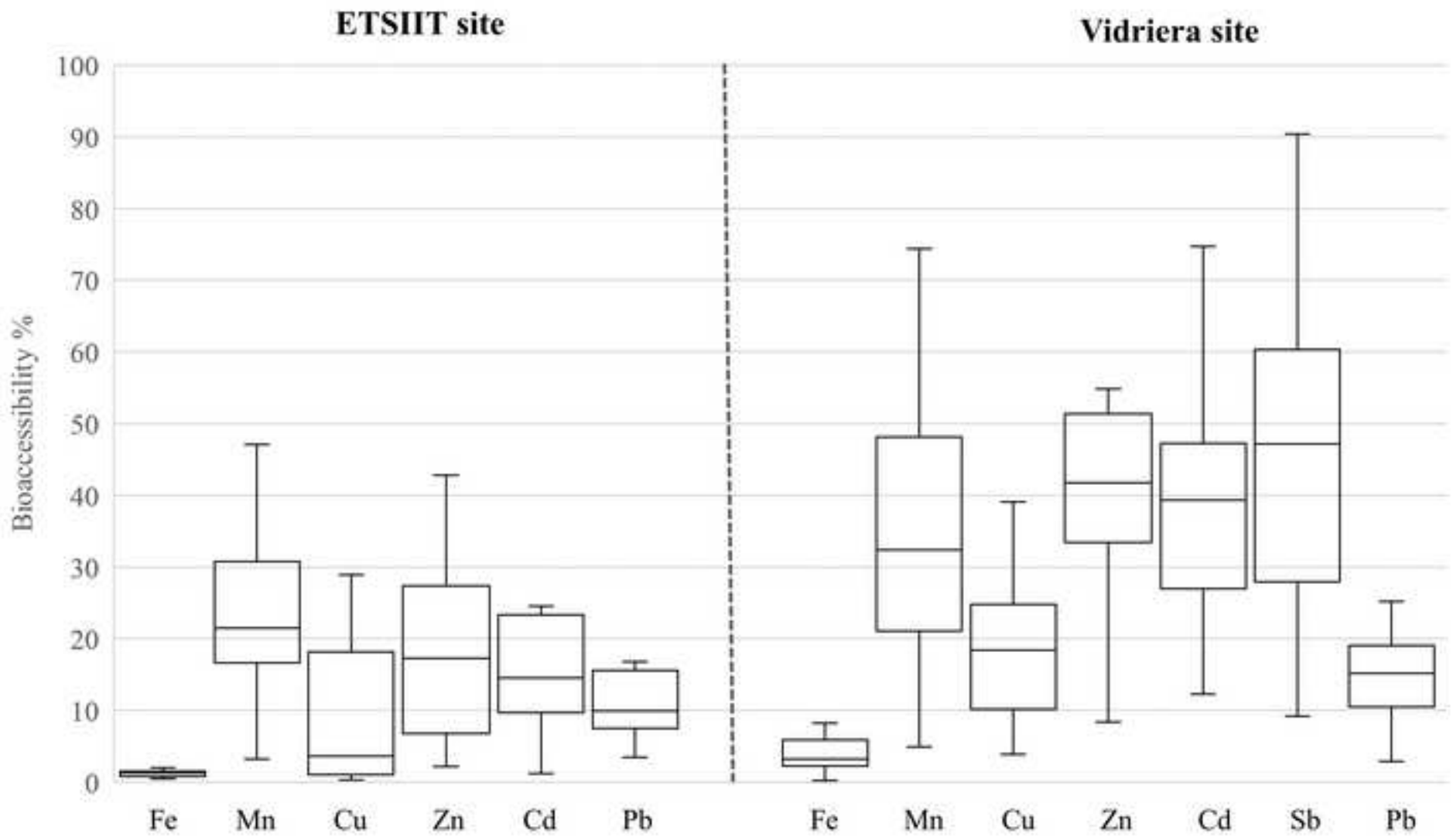

Figure 2

Click here to download high resolution image

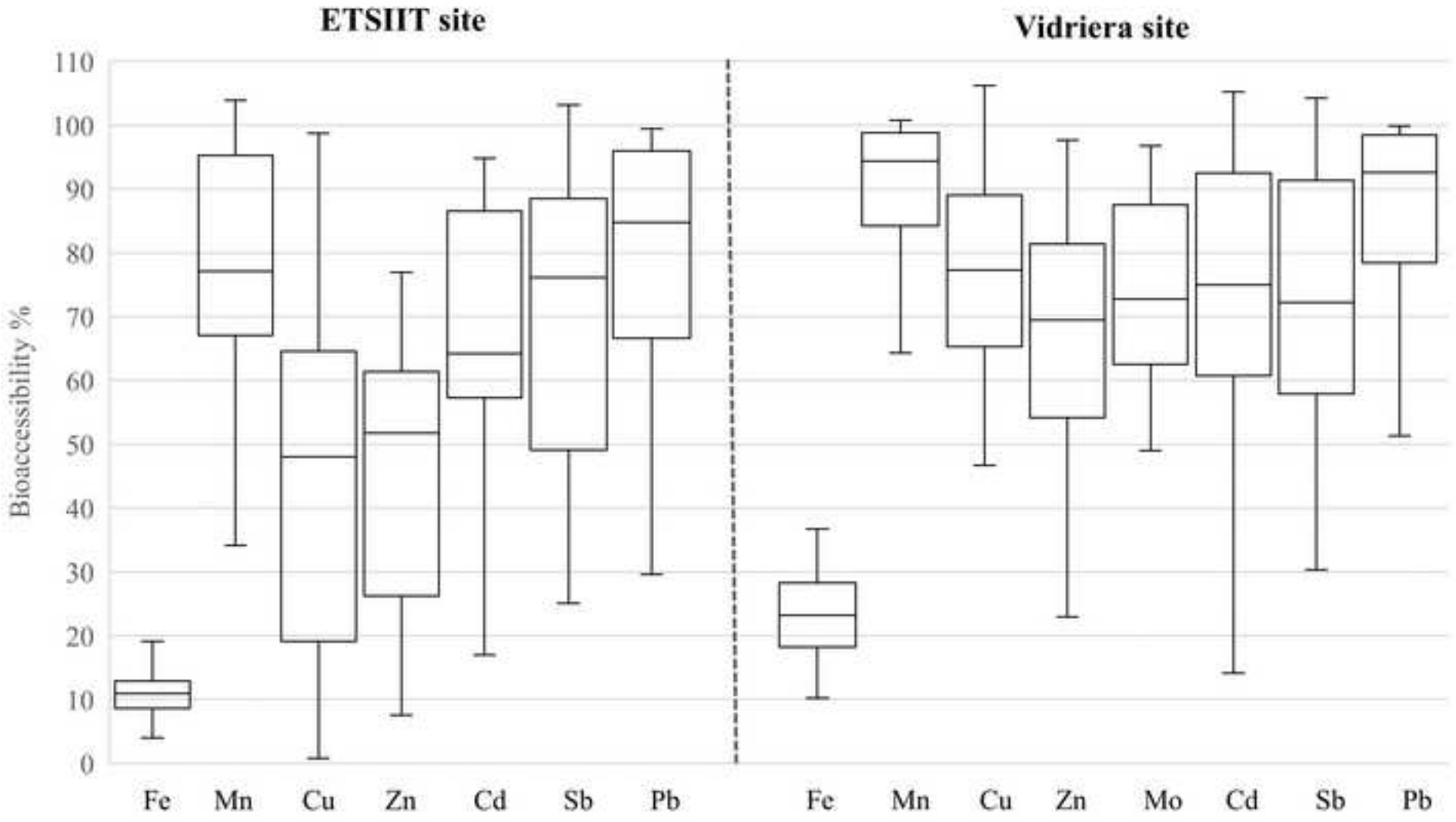

Figure S1

Click here to download Supplementary Material: Figure S1.jpg